# Improved compressed sensing and parallel MRI through the generalized series modeling

Xi Peng[1,2], Leslie Ying[3], Xin Liu[1,2], and Dong Liang[1,2]

[1]Paul C. Lauterbur Research Centre for Biomedical Imaging, Shenzhen Institutes of Advanced Technology, Shenzhen, Guangdong, China, [2]Key Laboratory of Health Informatics, Chinese Academy of Sciences, Shenzhen, Guangdong, China, [3]Department of Biomedical Engineering, Department of Electrical Engineering, The State University of New York at Buffalo, Buffalo, New York, United States

**INTRODUCTION:** The problem of reconstructing a high-spatial-temporal-resolution MR image sequence occurs in various MR applications, such as interventional imaging, dynamic contrast enhanced imaging, cardiac imaging, where a static reference image can be obtained with relative ease before the whole dynamic process. This work addresses the problem by integrating the generalized series (GS) model [1], in which the reference prior is incorporated, with standard compressed sensing (CS) [2] and parallel imaging (PI) [3] techniques. The proposed method was validated in a Monte-Carlo study and is shown to provide superior imaging quality with decreased g-factor to existing CS- and PI-based reconstruction methods.

**THEORY AND METHOD:** In the context of parallel acquisition, the GS model efficiently represents the multi-coil image function as a generalized-series expansion [4]: $\boldsymbol{\rho}_{GS}(\mathbf{r}, j) = \sum_{n=-M/2}^{n=M/2-1} \alpha_n(j)\varphi_n(\mathbf{r}, j)$, where $\alpha_n(j)$ denotes the GS coefficients for the j-th coil, M is the number of Nyquist samples at the central k-space and $\varphi_n(\mathbf{r}, j) = |\boldsymbol{\rho}_{REF}(\mathbf{r}, j)| \cdot \exp(i2\pi n\Delta\mathbf{k} \cdot \mathbf{r})$ are the GS basis functions incorporating a set of sensitivity-weighted reference priors. The GS coefficients for all coils can be directly jointly estimated by enforcing data consistency at the central k-space (grey rectangle in Fig. 1) with $\mathbf{D}_g$ and $\mathbf{y}_g$ denoting the corresponding sampling pattern and acquired data: $\boldsymbol{\alpha}_{GS} = \arg\min_{\boldsymbol{\alpha}_{GS}} \|\mathbf{D}_g\mathbf{F}\boldsymbol{\Phi}_{GS}\boldsymbol{\alpha}_{GS} - \mathbf{y}_g\|_2^2$ (1). The GS representation is very useful in modeling smooth contrast variations between the reference and target image, while it is less efficient in modeling localized discrepancies. To this end, we employ standard CS and PI technique to recover the residual image not captured by the GS model. Specifically, we use the SPIRiT [5] method as well as its regularized variant, and the proposed reconstruction (GS-SPIRiT-L1) can be formulated as:

$$\left(\boldsymbol{\alpha}_{GS}; \mathbf{x}\right) = \arg\min_{\boldsymbol{\alpha}_{GS}, \mathbf{x}} \|\mathbf{D}(\mathbf{F}\boldsymbol{\Phi}_{GS}\boldsymbol{\alpha}_{GS} + \mathbf{x}) - \mathbf{y}\|_2^2 + \lambda_1\|\mathbf{S}(\mathbf{G}_{resi} - \mathbf{I})\mathbf{x}\|_2^2 + \lambda_2\left(\mu\|\boldsymbol{\alpha}_{GS}\|_{1,2} + \|\boldsymbol{\Psi}_w\mathbf{F}^{-1}\mathbf{x}\|_{1,2}\right) \quad (2)$$

where $\mathbf{y}$ represents the acquired multi-coil k-space data, and $\mathbf{x}$ is the k-space data of the residual image. Operator $\mathbf{D}$ performs selection in the acquired k-space locations, $\|\cdot\|_{1,2}$ denotes the mixed $L_1$-$L_2$ norm (i.e., $\|\boldsymbol{\alpha}_{GS}\|_{1,2} = \sum_n \sqrt{\sum_j \|\alpha_n(j)\|^2}$) enforcing joint sparsity property on coefficients across coils, operator $\boldsymbol{\Psi}_w$ conducts a sparsifying transformation (i.e., wavelet), $\mu$ is a pre-determined constant to constrain the energy distribution between the GS representation and the residual image. $\lambda_1$ and $\lambda_2$ are regularization parameters. The sampling pattern is illustrated in Fig. 1. Other data acquisition schemes can also be designed. In Eq. (2), $\mathbf{G}_{resi}$ is the self-calibrating operator [5] convolving the k-space data of the residual image with appropriate calibration kernels. Deviating from the standard SPIRiT method, the calibration kernels are calculated only using the residual k-space data located in the central white area shown in Fig. 1. $\mathbf{S}$ is a binary mask designed to exclude the inconsistence introduced by the residual k-space data in the grey rectangle. It is worth noting that the standard SPIRiT and L1-SPIRiT are special cases of the proposed technique if we fix $\boldsymbol{\alpha}_{GS} = 0$ and set $\mathbf{S} = \mathbf{I}$. The SPIRiT and GS-SPIRiT reconstruction can be implemented via lease square (LSQR) algorithm. For the GS-SPIRiT-L1 method, we proposed to use an efficient projection over convex sets (POCS) algorithm described in Table 1, where operator $\mathbf{D}_c$ performs selection in the non-acquired k-space locations.
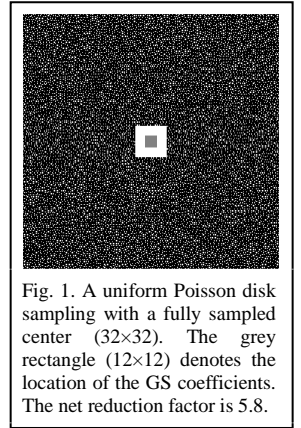


Fig. 1. A uniform Poisson disk sampling with a fully sampled center (32×32). The grey rectangle (12×12) denotes the location of the GS coefficients. The net reduction factor is 5.8.

**Table 1 GS-SPIRiT-L1 POCS Algorithm**

**Initialize:** estimate $\boldsymbol{\alpha}_{GS}^{(0)}$ using Eq. (1), calculate $\mathbf{G}_{resi}^{(0)}$,
$\qquad \mathbf{x}^{(0)} = \mathbf{D}^T(\mathbf{y} - \mathbf{DF}\boldsymbol{\Phi}_{GS}\boldsymbol{\alpha}_{GS}^{(0)})$, $k = 0$
**Iterate: 1.** $\mathbf{x}^{(k+1)} = \mathbf{G}_{resi}^{(k)}\mathbf{x}^{(k)}$,
$\qquad$ **2.** $\mathbf{x}^{(k+1)} = \mathbf{D}_c^T\mathbf{D}_c\mathbf{x}^{(k+1)} + \mathbf{D}^T(\mathbf{y} - \mathbf{DF}\boldsymbol{\Phi}_{GS}\boldsymbol{\alpha}_{GS}^{(k)})$,
$\qquad$ **3.** $\boldsymbol{\alpha}_w^{(k)} = \boldsymbol{\Psi}_w\mathbf{F}^{-1}\mathbf{x}^{(k+1)}$,
$\qquad$ **4.** $[\mu \cdot \boldsymbol{\alpha}_{GS}^{(k+1)}; \boldsymbol{\alpha}_w^{(k+1)}] = \text{JointSoftThresh}([\mu \cdot \boldsymbol{\alpha}_{GS}^{(k)}; \boldsymbol{\alpha}_w^{(k)}])$,
$\qquad$ **5.** $\mathbf{x}^{(k+1)} = \mathbf{D}_c^T\mathbf{D}_c\mathbf{F}\boldsymbol{\Psi}_w^{-1}\boldsymbol{\alpha}_w^{(k+1)} + \mathbf{D}^T(\mathbf{y} - \mathbf{DF}\boldsymbol{\Phi}_{GS}\boldsymbol{\alpha}_{GS}^{(k+1)})$,
$\qquad$ **6.** update $\mathbf{G}_{resi}^{(k+1)}$, $k = k+1$.
**Until convergence.**

**RESULTS AND DISCUSSION:** The proposed technique was validated via simulated data shown in Fig. 2. The target and reference images (256×256) are selected from a nine-image sequence of a variable flip-angle experiment. An eight-channel receive head coil (complex valued) was simulated based on the Biot-Savart's law [6]. To evaluate the noise behavior in the reconstruction, we conduct a Monte-Carlo study with 100 complex white Gaussian noise realizations. Regularization parameters are elaborately tuned to provide minimum reconstruction errors for each method. The LSQR and the POCS algorithms are implemented with 30 iterations. After reconstruction, the mean error and the empirical g-factor map are calculated. As can be seen, the SPIRiT method suffers from severe noise amplification and the largest reconstruction error, while the GS-SPIRiT method exhibits alleviated noise behavior. This is probably because for image content based parallel imaging techniques, such as SPIRiT, if a sparser data (the residual image in our case) is used to calculate the calibration kernel, the increased sparsity enables to lower the g-factor. The slightly increased error on the edges of the GS-SPIRiT reconstruction is mostly because of the decreased SNR and the reduced amount of calibration data. The L1-SPIRiT and the proposed GS-SPIRiT-L1 methods both successfully eliminate the noise amplification through L1 regularization. However, under the simulated conditions here (acceleration factor of 5.8 and noisy measurements), the proposed method exhibits less artifacts and preserves more image details.
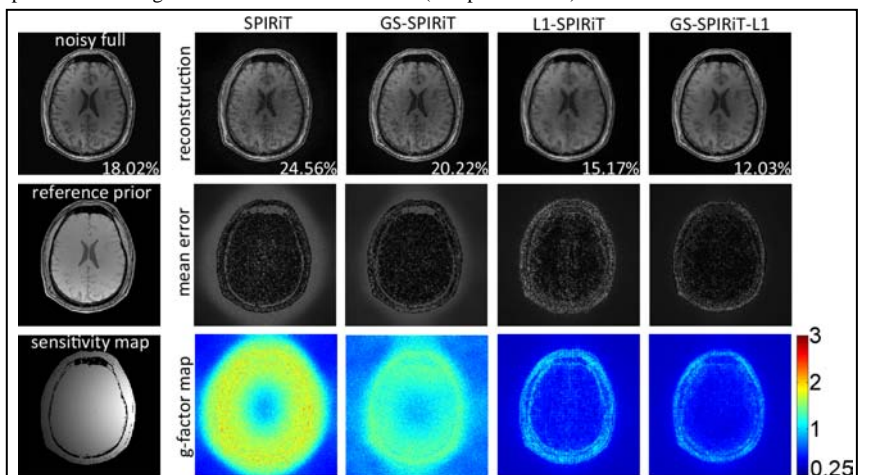


Fig. 2. Reconstruction results with a reduction factor of 5.8. Multi-coil images are combined with square root of sum of squares. The percentage number is the normalized MSE.

**CONCLUSION:** By integrating the generalized series model with standard compressed sensing and parallel imaging techniques, the proposed method achieves superior reconstruction quality with decreased g-factor to the state-of-art CS-PI based reconstruction methods from under-sampled noisy measurements.

**REFERENCE:** [1] Liang Z-P, *IEEE-TMI* 1994. pp. 677-686. [2] Lustig M, *MRM* 2007. pp. 1182-1195. [3] Ying L, *IEEE-SPM* 2010. pp. 90-98. [4] Liang Z-P, *ISMRM* 2003. pp. 2341. [5] Lustig M, *MRM* 2010. pp. 457-471. [6] Griffiths D. J, *Introduction to Electrodynamics* 1998.